Optimization-based strut-and-tie model generation for reinforced concrete structures under multiple load conditions

Xia, Yi; Langelaar, Matthijs; Hendriks, Max A.N.

DOI
10.1016/j.engstruct.2022.114501

Publication date
2022

Document Version
Final published version

Published in
Engineering Structures

Citation (APA)
Xia, Y., Langelaar, M., & Hendriks, M. A. N. (2022). Optimization-based strut-and-tie model generation for reinforced concrete structures under multiple load conditions. *Engineering Structures*, *266*, Article 114501. https://doi.org/10.1016/j.engstruct.2022.114501

Engineering Structures 266 (2022) 114501

Contents lists available at ScienceDirect

Engineering Structures

journal homepage: www.elsevier.com/locate/engstruct

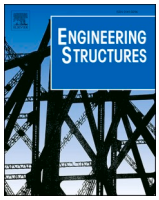

Optimization-based strut-and-tie model generation for reinforced concrete structures under multiple load conditions

Yi Xia [a,b,*], Matthijs Langelaar [c], Max A.N. Hendriks [d,e]

[a] School of Civil Engineering, Chongqing University, Chongqing 400045, China
[b] Key Laboratory of New Technology for Construction of Cities in Mountain Area of Ministry of Education, Chongqing University, Chongqing 400045, China
[c] Faculty of Mechanical, Maritime and Materials Engineering, Delft University of Technology, Delft, Netherlands
[d] Faculty of Civil Engineering & Geosciences, Delft University of Technology, Delft, Netherlands
[e] Department of Structural Engineering, Norwegian University of Science and Technology (NTNU), Trondheim, Norway

ARTICLE INFO

Keywords:
Reinforced concrete structures
Strut-and-tie
Multiple load combinations
Integrated optimization
Topology optimization
Nonlinear finite element analysis

ABSTRACT

Strut-and-Tie modelling (STM) has been widely applied to design D-regions of reinforced concrete structures. For economic and environmental reasons there is a need for optimized Strut-and-Tie models. How to optimize Strut-and-Tie models considering multiple load combinations has not been investigated extensively in the literature. In order to address this gap in this paper, we propose a method to generate multi-load optimization-based Strut-and-Tie (MOST) models to design D-regions under multiple load combinations. The proposed generation method involves the determination of basis vectors for the load combinations and generation of the corresponding optimization-based Strut-and-Tie models for each of the basis vectors by topology optimization and truss extraction. The generated model is then used to design D-regions under multiple load combinations. In order to check the effectiveness of the proposed method, three alternative approaches for multiple load combinations are investigated and discussed. These approaches comprise: (1) using manually created Strut-and-Tie models, (2) adopting multi-load topology optimization resulting in a single Strut-and-Tie model, (3) generating individual Strut-and-Tie models for each of the considered load combinations. In this paper, three 2D and one 3D D-regions are investigated to compare the effectiveness and applicability of the different methods. It is found that the proposed method results in more economical designs than the three alternative approaches.

1. Introduction

Reinforced concrete (RC) structures have been widely used in our society. It is always a challenge for engineers to design a safe and economical structure. This becomes even more important in developing a sustainability-oriented world. In order to propose effective methods, researchers have divided RC structures into two main regions: Bernoulli regions (B-regions) and Disturbed regions (D-regions). B-regions exhibit linear strain distributions in the cross section under external loads, whereas D-regions result in highly nonlinear strain distributions. Low slenderness and geometrical discontinuities are main reasons for the nonlinear strain distribution. Compared to B-regions, the nonlinearity of D-regions challenges engineers to select accurate and effective analytical methods for design. Among various approaches, the Strut-and-Tie modelling (STM) method has been widely applied to design D-regions of reinforced concrete for over two decades [4]. After years of research on the STM method, it has been recommended in various design codes in practice, including [13,14,3,9,2].

The STM method is a truss-analogy method initially proposed by Ritter [34] and Mörsch [30] in the early twentieth century, and further generalized as a consistent design method by Schlaich et al. [36] and Schlaich and Schäfer [35]. In STM analysis, the complex force transfer mechanism is simplified by using a given truss-like model. The obtained information, such as axial equilibrium forces, member locations and simulated stress states, support engineers to analyze and design complex D-regions. The STM method is based on the lower bound plasticity theory [29,5,50,31], and results in safe RC designs.

In the standard STM method, the first step is to determine a suitable truss system to analogize the load transfer mechanism in the D-region and calculate the corresponding equilibrium forces. The next step is to determine the minimum required cross-sectional area of steel reinforcement bars and to verify the concrete strength of struts and nodes.

* Corresponding author at: School of Civil Engineering, Chongqing University, Chongqing 400045, China.
E-mail address: yi_xia@cqu.edu.cn (Y. Xia).

https://doi.org/10.1016/j.engstruct.2022.114501
Received 27 January 2022; Received in revised form 28 April 2022; Accepted 30 May 2022
Available online 24 June 2022

The last step is to detail the steel layout considering practical requirements. The simple implementation of this method and the resulting safe designs are preferred characteristics in practice. However, there are still some difficulties in applying the STM method, such as, finding suitable truss-like models [48,25,19,18], determining accurate safety factors [42,33], and considering complex dynamic loadings [37]. Some challenges in STM have been summarized in Tjhin and Kuchma [43].

Among these issues, determining a suitable truss-like model is of vital importance. This problem becomes even more important in reinforcement design based on the STM method considering multiple load combinations. This topic is the main focus of this paper and the context will be introduced after discussing the developments towards automated Strut-and-Tie (ST) model generation. Suitable truss analogy models are commonly created by experienced engineers who have sufficient structural insight into the designed D-regions. However, with the increased complexity of D-regions, it is more difficult for engineers to find a suitable truss-like model to guarantee the structural performance of the resulting design [12,6,26,32]. In order to generate suitable ST models, various topology optimization (TO) methods have been adopted, e.g., the ESO (evolutionary structural optimization) methods [26,27,1,16,23], the BESO (Bi-directional ESO) method [38,37], the SIMP (solid isotropic material with penalization) methods [6–8,21] and other methods [45,20,15]. The obtained results of the proposed TO methods have been systematically evaluated in the perspective of the STM method in our previous study [48]. Compared to the manual STM generation based on a trail-and-error process and designer's intuition, TO methods automatically and systematically provide the optimization results which could be used as the draft to generating ST models. The resulting accuracy of the STM in indicating load transfer mechanism is improved and the required manual efforts are reduced. An important problem was identified that suitable Strut-and-Tie (ST) models cannot be directly generated without manual adjustments. In order to solve this problem, we previously proposed a method to automatically generate the optimization-based strut-and-tie model (OPT-STMs) in Xia et al. [47]. Furthermore, this proposed method was extended in Xia et al. [49] to generate OPT-STMs for 3D D-regions, but all for a single loading scenario.

In the current STM investigations, the research mainly focuses on structures under a single load combination, in which loads are assumed to act on a structure simultaneously and increase proportionally. However, in practice, the safety and performance of the designed structures need to be checked considering several load combinations. These load combinations could contain the permanent loads and accidental loads, such as self-weight, traffic loads, seismic loads and wind loads. It is an important safety aspect for a systematic STM approach to consider multiple load combinations in the design process. Very few investigations have been conducted in this regard. Shobeiri and Ahmadi-Nedushan [38] used the BESO method generate 3D STMs considering multiple load conditions. In this method, these loads were taken as several single-load cases to generate STM individually. Bruggi [7] adopted a multi-load TO formulation to obtain optimized topologies considering the interaction of multiple load combinations. The obtained TO results could be used as inspiration for the generation of ST models which are suitable under multiple load combinations. The load condition of torsional moments was also investigated in these studies. However, to what extent the obtained topologies are effective for the generation of ST models considering multiple load combinations has not been investigated. For the practical application of STM, how to obtain an ST model which provides safe and effective structural performance in case of multiple load combinations is still one of the important problems.

In order to solve this problem, in this paper, we propose a method to generate multi-load OPT-STMs (abbreviated as MOST) to obtain safe and effective designs under the considered multiple load combinations. In this approach, the considered load combinations are decomposed into a set of basis vectors: these basis vectors comprise load combinations themselves, which are linearly independent and span all considered load combinations. By decomposing the load combinations in this way, the TO of each basis vector results in topologies that are more amendable to truss extraction. In addition, since linear analysis is used in the STM dimensioning process, the ST models belonging to each basis vector can be superimposed and design can be conveniently performed according to the actual set of load combinations. The optimization-based Strut-and-Tie models (OPT-STMs), which result in economical and safe designs compared to traditional models, with respect to each load combination basis are created based on our previously proposed generation methods [47,49]. The generated OPT-STMs thus represent several independent load transfer mechanisms, equal to the number of basis vectors. The MOST model is then generated by superimposing these models to capture load transfer mechanisms for multiple load combinations. The equilibrium forces and member locations can be obtained based on the obtained MOST model under the considered load combinations, and they are used for designing the structure.

In addition, three other possible methods for the STM problem under multiple load combinations are investigated. They are: (1) creating manual ST models; (2) generating multiple models for each considered load combination; (3) applying multi-load TO formulation [7] in the generation of ST model. Through four case studies, both in 2D and 3D, the obtained results of the investigated procedures are compared. The effectiveness of the proposed approach is validated. Based on the evaluated structural performance and steel usage, the question which method leads to the most economical designs is addressed. Note that, practical implementation aspects, such as steel detailing and constructability, are not considered in this paper.

The remaining contents are organized as follows: Section 2 introduces the details of the four investigated methods. Section 3 presents an illustrative deep beam case to illustrate the main steps of the investigated methods and their comparisons in terms of capacity and steel usage. Section 4 conducts reinforcement design for two 2D and one 3D D-regions. Three manually created ST models are proposed to compare the performance of the MOST design in the investigated cases. Section 5 further discusses the application of other two procedures (using multiple OPT-STMs and applying multi-load TO formulation leading to one single ST model) in STM under multiple load combinations, and demonstrates various difficulties that arise in these methods. Finally, the conclusions of this paper are given in Section 6.

2. Strut-and-Tie design approaches considering multiple load combinations

In this section, four approaches for STM design under multiple load combinations are introduced. The flowchart of the four approaches is shown in Fig. 1. The first approach is manually creating an ST model for all considered load combinations. The second approach generates multiple ST models, one for each considered load combinations. The third approach uses the ML-TO formulation [7] for the STM generation. The last approach is the proposed MOST generation method. The details of the investigated approaches are introduced in the following subsections.

In this paper, Eq.(1) defines the i-th load combination for a specific design problem.

$$C_i = \{\psi_{ij} L_j (j = 1, ..., k)\} (i = 1, ..., n), \tag{1}$$

where C_i indicates the i-th of n considered load combinations.L_j indicates corresponding loadings, such as vertical and horizontal forces. ψ_{ij} defines the representative load factors of these loadings and can be zero for specific load combinations. In this paper, the finite element method (FEM) is applied in the generation and evaluation process. Nodal forces are applied for each considered loading L_j(notation as in Eq. (1)), thus, the discretized load combination can be defined as:

$$C_i = \sum_{j=1}^{k} \psi_{ij} L_j (i = 1, ..., n), \tag{2}$$

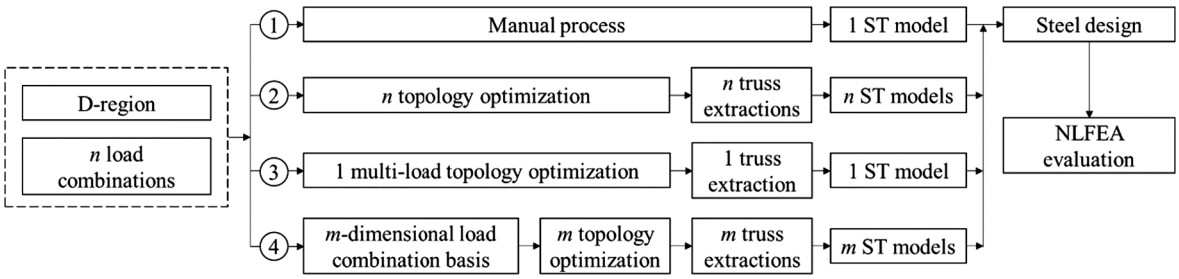

Fig. 1. Flowchart of four STM design procedures considering multiple load combinations. Approach ① indicates usage of a manually created ST model. Approach ② generates n ST models with respect to n load combinations for designing. Approach ③ applies the multi- load TO formulation to generate suitable ST model. Approach ④ shows the proposed MOST model generation method containing m ST models.

where $\mathbf{L}_j$ indicates nodal forces for the corresponding loading. In order to illustrate the details of the four approaches, a deep beam study is presented in Section 3.

2.1. Approach ①: Manually created ST model

In the STM design process, creating models manually is common in practice. Researchers have proposed various manually created ST models for several D-regions, such as, anchorage zones [17], pile caps [11], deep beams [10,24]. The creation of ST models depends on engineers' experience and insight, which is difficult for nonstandard D-regions. The manual process leads to varying quality of the resulting STM design. The created models do not need to be stable structures. However, it is necessary for engineers to obtain axial equilibrium forces based on the created models. The obtained equilibrium forces are then used to design the investigated D-regions.

In STM design considering multiple load combinations, the created model must exhibit purely axial equilibrium forces under all the considered combinations. Compared to the single-load design problem, the generation of suitable ST models becomes even more difficult. In order to satisfy the STM requirement, in this paper, a stable truss is used as a ST model. Stable truss structures can provide axial equilibrium forces under multiple load combinations. The maximum tensile member forces can be determined based on the calculation for all the considered load combinations. Based on the calculated maximum tensile forces, one can design the required rebar size.

2.2. Approach ②: Generation of ST models corresponding to multiple load combinations

In the previous approach of the manually created ST model, only one truss model is created. Here, another approach is directly generating multiple ST models with respect to each of the considered load combinations to design D-regions. To et al. [44] and Sritharan [41] proposed two ST models for two load combinations to investigate a tee joint case. Shobeiri and Ahmadi-Nedushan [38] used the BESO method to generate several ST models to investigate 3D D-regions under different loadings. The proposed ST models indicate different load transfer mechanisms.

In this paper, we apply the previously proposed OPT-STM generation method [47,49] to generate multiple models for the considered load combinations. The generated OPT-STMs are obtained via three phases, the topology optimization phase, the topology extraction phase and the STM shape optimization phase. A deep beam which will be investigated in Section 3 is used to introduce the generation process, as shown in Fig. 2. The generated model indicates an effective load transfer mechanism for the considered loading. Based on the previous evaluation, compared to manually created ST models, the generated OPT-STMs show sufficient loading capacity and result in the most economical steel usage.

In this paper,$\Phi(\cdot)$ indicates the OPT-STM generation process and $\Phi(\mathbf{C}_i)$ represents the generated ST model with respect to load combination $\mathbf{C}_i$. For n considered load combinations, n OPT-STMs $\{\Phi(\mathbf{C}_i)\ \ (i = 1, \ldots, n)\}$ are generated. Similar to the process of applying the manual model, the obtained member forces based on the generated OPT-STMs are used to design the required reinforcement. The final design considering multiple load combinations can be obtained by determining reinforcement for each load combination $\mathbf{C}_i$ based on $\Phi(\mathbf{C}_i)$ and superimposing the calculated reinforcements corresponding to the different load combinations. The struts are assumed to have sufficient capacity, which will be checked using NLFEA simulation in Section 3.5.

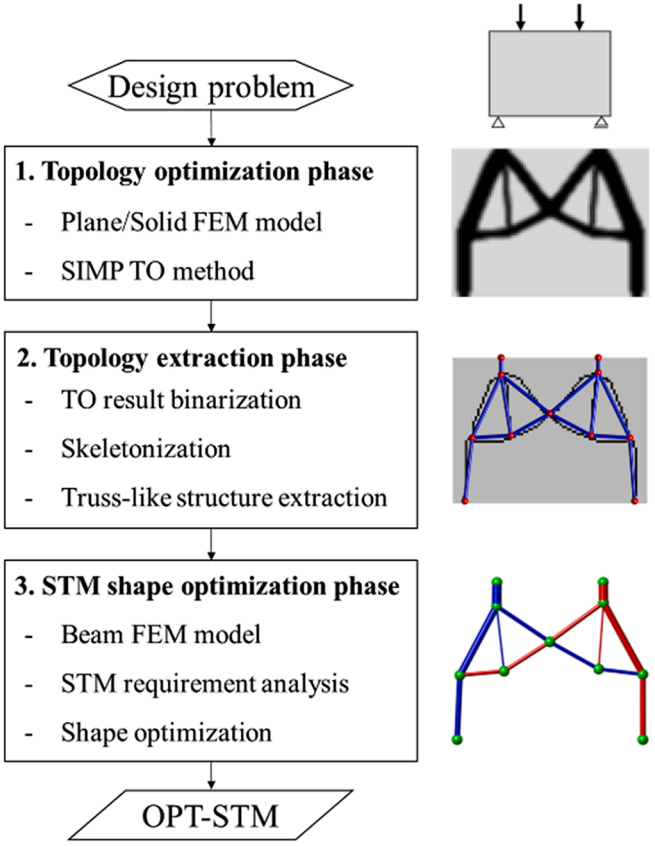

Fig. 2. Flow chart of the OPTSTM generation method [47,49]. A deep beam is used to illustrate the three phases. A full example is discussed in Section 3.

2.3. Approach ③: Multi-load topology optimization based STM generation method

Generating optimized material layouts considering multiple loadings have been broadly investigated in the TO field, e.g., Zhou and Li[51]; Sigmund [40],Zhuang et al. [52],Lógó et al. [28]. However, few

investigations have been conducted into STM generation considering multiple load combinations. Bruggi [7] applied the multi- load TO formulation and generated optimized layouts. The interaction of multiple loading combinations is considered in the optimization process and results in a single TO result. However, in this study the ST model was extracted by manual interpretation of the TO result. For systematic design, free from subjective choices, an automated approach is desired. In this paper, we incorporate the multi-load TO formulation and the OPT-STM generation method [47,49] to further investigate the applicability of the multi-load TO formulation in STM. For completeness the formulation of the multi-load TO method considering the multiple load combinations is briefly introduced in Appendix.

$\Phi_m(\cdot)$ indicates the modified OPT-STM generation process regarding the multi-load topology optimization. For n considered load combinations, this process generates one ST model for designing. For a given load combination $\mathbf{C}_i = \sum \psi_{ij}\mathbf{L}_j$, axial equilibrium forces and member locations can be calculated based on the obtained model, as $\Phi_m(\mathbf{C}_i)$. Subsequently, the required steel usage can be designed by accounting for the maximum tensile forces per truss element under all the considered load combinations.

2.4. Approach ④: Multi-load optimization-based STM generation method

Apart from the previous three methods, a novel method is proposed to generate MOST models for multiple load combinations. In the proposed method, a set of basis vectors is firstly determined by decomposing the considered load combinations. All considered load combinations can be obtained via linear combination of these basis vectors, which represent independent characteristic loadings for the considered set of load combinations. Next, for each determined basis vector a corresponding OPT-STM can be generated. The obtained models indicate independent, effective load transfer mechanisms. Lastly, the MOST model is generated by superimposing these obtained OPT-STMs, which enables to represent various load transfer mechanisms for multiple load combinations.

2.4.1. Determination of load combination basis

For the considered load combinations, shown in Eq. (2), it can be written in a matrix form as in Eq. (6).

$$\mathbf{C} = \Psi\mathbf{L} \tag{6}$$

Here $\mathbf{C}$ is a matrix containing all load combination vectors $\mathbf{C}_i$ and $\mathbf{L}_i$ is a matrix containing all load combination vectors L_j.Ψ indicates the load combination relation matrix with elements of loading factors ψ_{ij}.

A basis vector is determined by considering the load interactions and decomposing the considered load combinations. In this paper, we apply the reduced row echelon form to the load combination relation matrix Ψ, as shown in Eq. (7).

$$\Psi \overset{\text{RREF}}{\rightarrow} \overline{\Psi} :\Rightarrow \mathrm{B}_i \quad (i = 1, \ldots, m) \tag{7}$$

$\overline{\Psi}$ indicates the reduced matrix. The rank of $\overline{\Psi}$ indicates the number of the determined basis vectors. The rows of $\overline{\Psi}$ indicate m basis vectors (B_i).

The determined basis decomposes the considered load combinations. The number of determined basis vectors B_i is always smaller or equal to the number of load combinations $\mathbf{C}_i$, $m \leqslant n$. All considered load combinations can be represented by the basis vectors via a linear combination in Eq. (8).

$$\mathbf{C} = \Psi'\mathbf{B} \tag{8}$$

In this equation,Ψ' is the load combination relation matrix corresponding to the determined basis vectors $\mathbf{B}$.

2.4.2. Model generation and reinforcement design

Based on the calculated basis vectors B_i, the generation process $\Phi(\cdot)$ similar in Section 2.2 is used to generate effective models. The corresponding OPT-STM ($\Phi(\mathrm{B}_i)$) is generated for each determined basis vector B_i. The resulting m models indicate independent load transfer mechanisms. The axial equilibrium forces and member locations can be obtained based on the generated models. The proposed multi-load optimization-based Strut-and-Tie (MOST) model under multiple load combinations is composed by multiple OPT-STMs ($\Phi(\mathrm{B}_i)$). In the composite model, the supported and loaded nodes are shared while the rest of each truss structure is modelled independently. Subsequently, the generated MOST model is used to determine equilibrium forces under the considered load combinations $\mathbf{C}_i$.

There are two main features of the generated MOST models. Firstly, the generated MOST model is applicable for varying loadings including the change of magnitudes and directions. This feature makes the MOST model is applicable for the design of various load combinations in a convenient manner. Secondly, the basic OPT-STMs ($\Phi(\mathrm{B}_i)$) indicate independent load transfer mechanisms. This feature enables the design under multiple load combinations via several basic models. The details of these two features are further introduced through an illustrative example in Section 3.4.3.

3. Illustrative deep beam

In this section, a deep beam considering multiple load combinations is designed via the four approaches. The geometry, boundary and loading conditions of the deep beam are shown in Fig. 3. In this deep beam, $\mathbf{L}_1$ and $\mathbf{L}_2$ represent the vertical loading of 300 kN and horizontal loading of 100 kN, respectively. $\mathbf{L}_3$ represents the bending moment of 250 kN • m acting on the top. The discretized forces of three loadings are shown in Fig. 4. In this case, four load combinations $\mathbf{C}$ are considered, as shown in Table 1, and ψ is a binary matrix.

In the generation process, the finite element model is firstly created. The deep beam is discretized by 80 × 60 four-node bilinear plane stress elements. In the optimization process, the volume fraction is taken as 30 % and the filter radius is 2× mesh size. TO is a non-convex optimization problem with many local optima. By changing the volume fraction and filter radius, different locally optimal results are obtained. The influence of these parameters has been investigated in our previous investigation [47]. The resulting OPT-STM has a stable structural performance within a range of parameters. The results of the four generation methods are presented below. Lastly, the resulting designs are simulated by Nonlinear Finite Element Analysis (NLFEA) to evaluate their

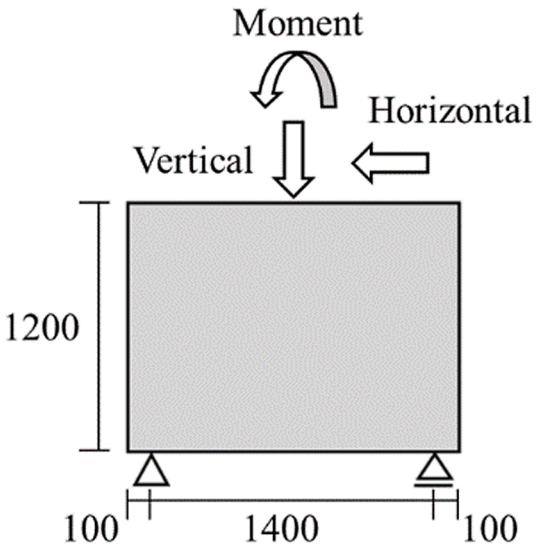

Fig. 3. Geometry and loadings of the simple supported deep beam (mm). The thickness of the deep beam is 100 mm.

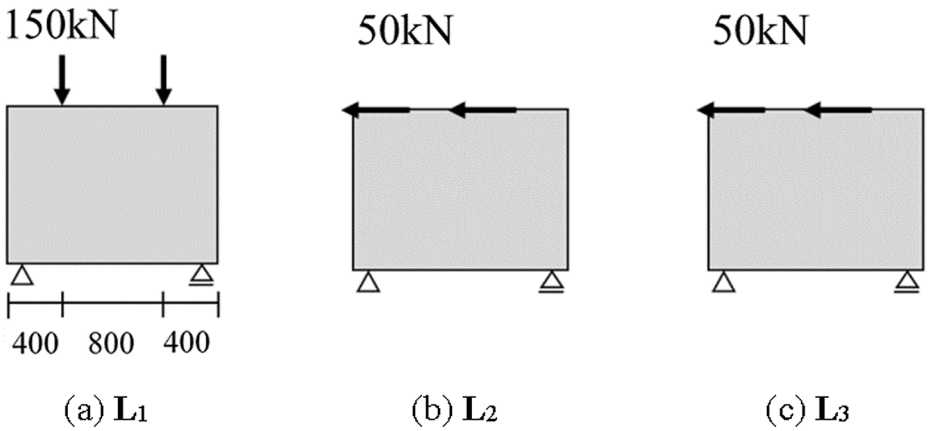

Fig. 4. Three discretized loads of the deep beam. L1, L2 and L3 indicate vertical, horizontal and moment loadings, respectively.

Table 1
Four considered load combinations for designing the deep beam.

No.	Load combinations
$\mathbf{C}_1$	$\mathbf{L}_1 + \mathbf{L}_2$
$\mathbf{C}_2$	$\mathbf{L}_1 + \mathbf{L}_3$
$\mathbf{C}_3$	$\mathbf{L}_2 + \mathbf{L}_3$
$\mathbf{C}_4$	$\mathbf{L}_1 + \mathbf{L}_2 + \mathbf{L}_3$

performance, further details are provided in Section 3.5. In this paper, the yield strength of steel is set to 580 MPa.

3.1. Manually created model

Since no prior information is found for the generation of ST models for the deep beam under multiple load combinations, we create a stable truss to form the model. The manually created model of Approach ① is shown in Fig. 5. The stable truss enables calculation of equilibrium forces under multiple load combinations. The resulting equilibrium forces for the four load combinations ($\mathbf{C}_i$ (i = 1, 2, 3, 4)) are shown in Fig. 6. The required steel cross-sections based on the manual model are shown Fig. 7.

3.2. Generated model based on multiple OPT-STMs

In Approach ②, four OPT-STMs ($\Phi(\mathbf{C}_i)$) are generated with respect to the considered load combinations $\mathbf{C}_i$ (i = 1, …, 4). The optimized topologies are shown in Fig. 8. The resulting generated OPT-STMs ($\Phi(\mathbf{C}_i)$) are shown in Fig. 9. The STS indices with respect to four load combinations are {0.99, 0.98, 0.98, 0.99}. The reinforcement design can proceed based on these generated models, and the resulting rebar sizes are shown Fig. 10.

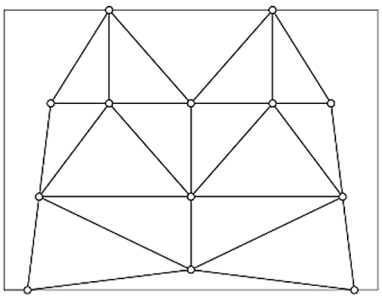

Fig. 5. The manually created ST model of the deep beam considering multiple load combinations.

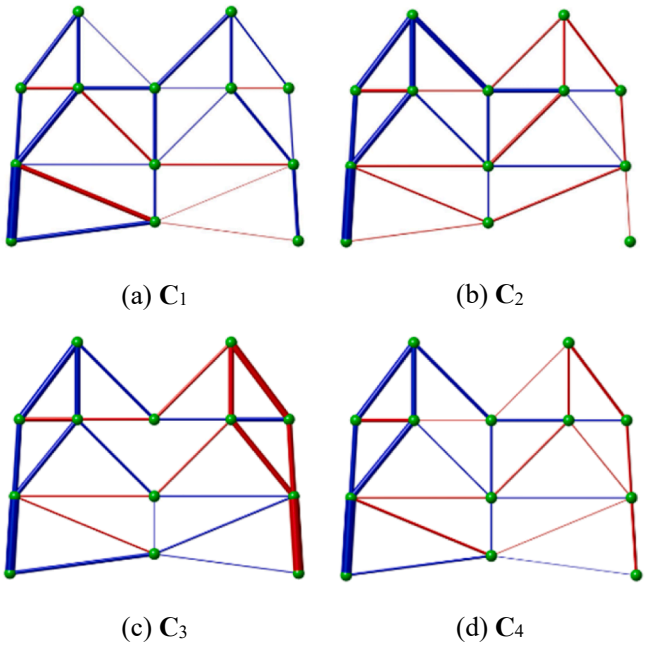

Fig. 6. Obtained member forces based on the manually created model. Red and blue members indicate ties and struts respectively. Bar width indicates the force magnitude. Members with forces lower than 1 % of the maximum force are not displayed. (For interpretation of the references to colour in this figure legend, the reader is referred to the web version of this article.)

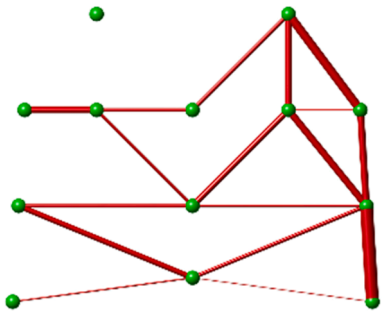

Fig. 7. Required steel cross-sections based on the manually created model. Bar width indicates the rebar cross-section.

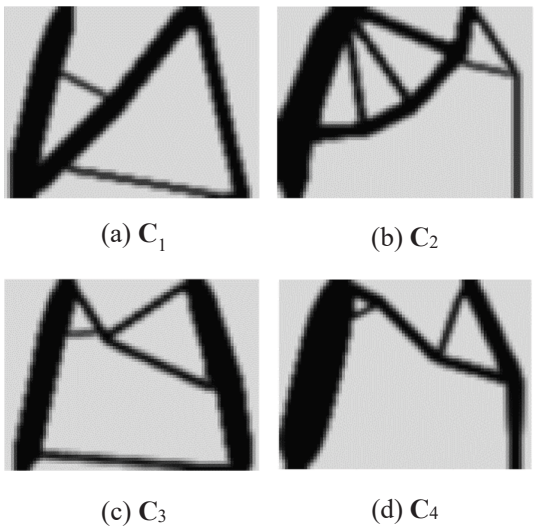

Fig. 8. Optimized topologies with respect to the considered load combinations.

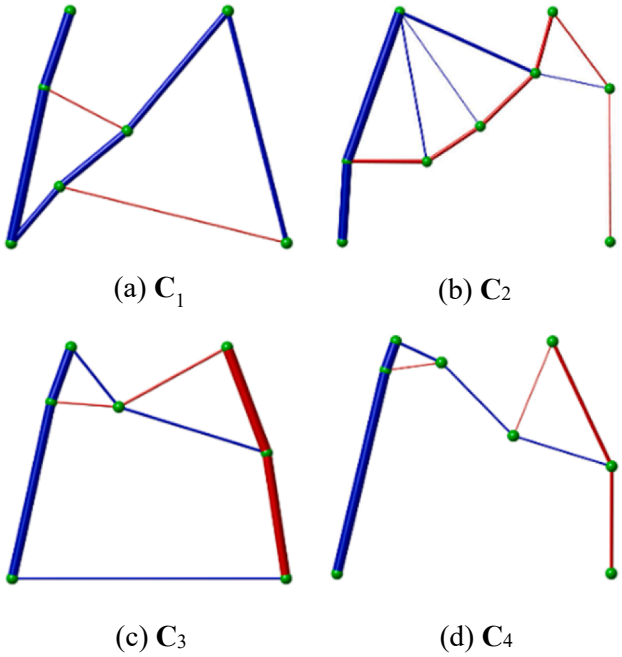

Fig. 9. Generated OPT-STMs with respect to the considered load combinations. Red and blue members indicate ties and struts respectively. Bar width indicates the force magnitude. Members with forces lower than 1 % of the maximize force are not displayed. (For interpretation of the references to colour in this figure legend, the reader is referred to the web version of this article.)

3.3. Multi-load topology optimization based model generation

In Approach ③, multi-load TO is performed to obtain the optimized layout as shown in Fig. 11. For the obtained TO result, a truss-like structure is extracted and the STM shape optimization (see in Eq.(4)) is conducted. The resulting ST model is shown in Fig. 12. The STS indices of the OPT-STM with respect to the four load combinations are {0.96, 0.96, 0.97, 0.99}, which guarantees the required axial force equilibrium. The member forces of the obtained model under these load combinations are shown in Fig. 13. The obtained tensile forces are then used to design reinforcement under multiple load combinations. The required steel cross-sections based on the generated model are shown Fig. 14.

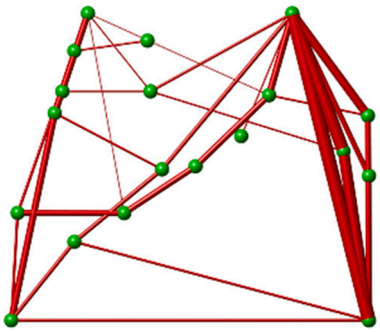

Fig. 10. Required steel cross-sections based on the generated OPT-STMs.

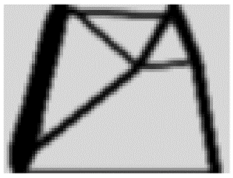

Fig. 11. Optimized material distribution of the multi-load topology optimization for the deep beam.

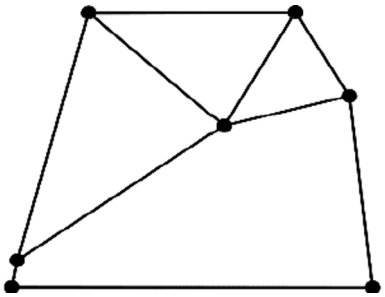

Fig. 12. The generated OPT-STM based on multi-load topology optimization result for the deep beam.

3.4. Multi-load optimization-based Strut-and-Tie model

In this section, the features of the proposed MOST method ④ are introduced through this illustrative deep beam. Firstly, the basis vectors for the considered load combinations are determined. The determination process is also applied on a more complex situation for further demonstration of the procedure. Secondly, the ML-OPT-STM is generated by combining several ST models with respect to basis vectors. The applicability and resulting independent load transfer mechanisms of the generated ML-OPT-STM are demonstrated.

3.4.1. Basis vector determination

Table 1 shows the considered load combinations for this deep beam. Considered load combinations $\mathbf{C}_i$ and loadings $\mathbf{L}_i$ can be formulated in matrix form in Eq. (9).Ψ is the corresponding load combination relation matrix. Each of the four considered load combinations $\mathbf{C}_i$ is a linear combination of three loadings $\mathbf{L}_i$.

$$\mathbf{C} = \Psi\mathbf{L} = \begin{bmatrix} 1 & 1 & 0 \\ 1 & 0 & 1 \\ 0 & 1 & 1 \\ 1 & 1 & 1 \end{bmatrix} \begin{bmatrix} \mathbf{L}_1 \\ \mathbf{L}_2 \\ \mathbf{L}_3 \end{bmatrix} \tag{9}$$

Based on the load combination relation matrix Ψ, we can obtain its reduced row echelon form Ψ_r shown in Eq. (10). The basis vectors $\mathbf{B}$ can be calculated by the matrix product shown in Eq. (11). In this case, we can obtain three corresponding basis vectors $\mathbf{B}_i$ of $\{\mathbf{L}_1\}$, $\{\mathbf{L}_2\}$ and $\{\mathbf{L}_3\}$.

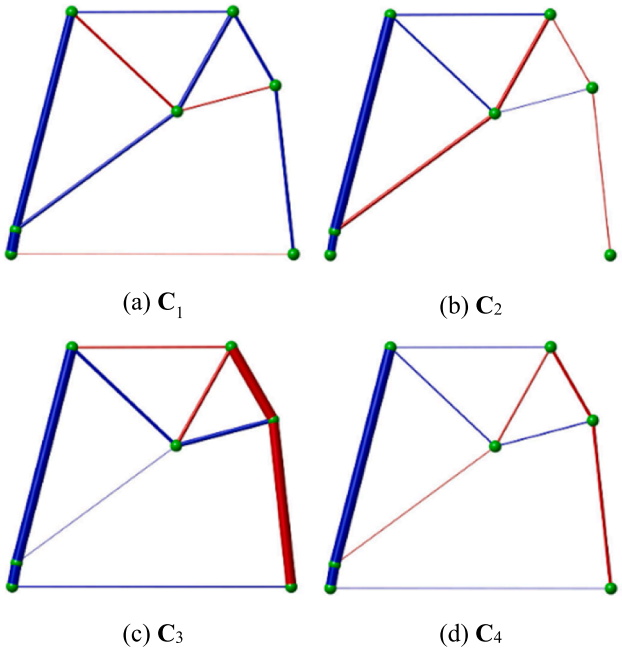

Fig. 13. Obtained member forces based on the model using multi-load topology optimization. Red and blue members indicate ties and struts respectively. Bar width indicates the force magnitude. Members with forces lower than 1 % of the maximize force are not displayed. (For interpretation of the references to colour in this figure legend, the reader is referred to the web version of this article.)

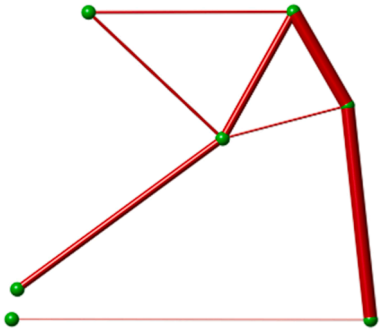

Fig. 14. Required steel cross-sections based on the generated OPT-STM adopting multi-load TO formulation.

$$\Psi \overset{\text{RREF}}{\rightarrow} \Psi_r = \begin{bmatrix} \mathbf{1} & 0 & 0 \\ 0 & \mathbf{1} & 0 \\ 0 & 0 & \mathbf{1} \\ 0 & 0 & 0 \end{bmatrix} \tag{10}$$

$$\mathbf{B} = \Psi_r \mathbf{L} \tag{11}$$

Before continuing with the model generation, for illustration also a situation with more loadings and load combinations is presented. A tee joint case, which will be investigated in Section 4.2, is taken as an example. Six loadings act on this joint, shown in Fig. 15. Six considered load combinations with various load factors ψ_{ij} are shown in Table 2. The resulting load combination relation matrix Ψ and its reduced form Ψ_r are shown in Eq. (12). In this case, the rank of this matrix is four and the resulting basis vectors $\mathbf{B}_i$ are $\{\mathbf{L}_1 + \mathbf{L}_2\}$, $\{\mathbf{L}_3\}$, $\{\mathbf{L}_4 + \mathbf{L}_5\}$ and $\{\mathbf{L}_6\}$. Note that, the number of basis vectors is smaller than the considered load combinations.

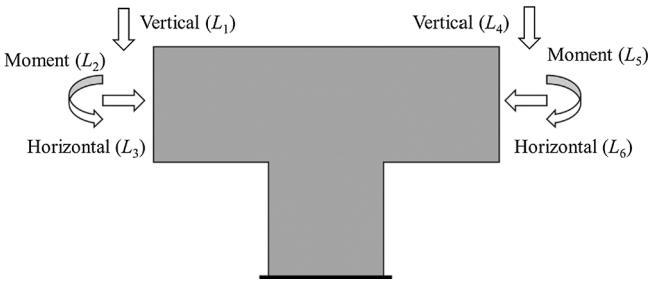

Fig. 15. Geometry and loadings of the illustrative tee joint case.

Table 2
Six considered load combinations of the tee joint. Symbol − in the load combinations indicates the opposite load direction.

No.	Load combinations
$\mathbf{C}_1$	$\mathbf{L}_1 + \mathbf{L}_2$
$\mathbf{C}_2$	$\mathbf{L}_1 + \mathbf{L}_2 + 1.5\mathbf{L}_3$
$\mathbf{C}_3$	$\mathbf{L}_4 + \mathbf{L}_5$
$\mathbf{C}_4$	$\mathbf{L}_4 + \mathbf{L}_5 + 1.5\mathbf{L}_6$
$\mathbf{C}_5$	$1.35\mathbf{L}_1 + 1.35\mathbf{L}_2 + \mathbf{L}_3 + 1.35\mathbf{L}_4 + 1.35\mathbf{L}_5 + \mathbf{L}_6$
$\mathbf{C}_6$	$1.2\mathbf{L}_1 + 1.2\mathbf{L}_2 - \mathbf{L}_3 + 1.2\mathbf{L}_4 + 1.2\mathbf{L}_5 - \mathbf{L}_6$

$$\Psi = \begin{bmatrix} 1 & 1 & 0 & 0 & 0 & 0 \\ 1 & 1 & 1.5 & 0 & 0 & 0 \\ 0 & 0 & 0 & 1 & 1 & 0 \\ 0 & 0 & 0 & 1 & 1 & 1.5 \\ 1.35 & 1.35 & 1 & 1.35 & 1.35 & 1 \\ 1.2 & 1.2 & -1 & 1.2 & 1.2 & -1 \end{bmatrix} \overset{RREF}{\longrightarrow} \overline{\Psi}$$
$$= \begin{bmatrix} 1 & 1 & 0 & 0 & 0 & 0 \\ 0 & 0 & 1 & 0 & 0 & 0 \\ 0 & 0 & 0 & 1 & 1 & 0 \\ 0 & 0 & 0 & 0 & 0 & 1 \\ 0 & 0 & 0 & 0 & 0 & 0 \\ 0 & 0 & 0 & 0 & 0 & 0 \end{bmatrix} \tag{12}$$

3.4.2. Generation of MOST model

Based on the obtained basis vectors of the deep beam, three OPT-STMs ($\Phi(\mathbf{B}_i)$) are generated accordingly. The generated OPT-STMs each indicate an independent load transfer mechanism with respect to the load combination basis. In the generation method, the obtained TO results and the resulting OPT-STMs are shown in Fig. 16. The STS indices of the OPT-STMs under three basis vectors are 0.99, 0.98 and 0.99 respectively. The obtained basic models form the MOST model to design the structure under multiple load combinations. The resulting steel design is shown in Fig. 17.

3.4.3. Two main features in the generated MOST model

Here, two main features of the generated model based on the basis vectors are introduced. Firstly, the generated OPT-STM is applicable for all ranges of load magnitude within the corresponding basis vector, including the change of loading directions. In case of considering more load combinations, when the added load combinations can be represented by the existing basis vectors, the obtained basis vectors remain unchanged. Moreover, the obtained OPT- STM ($\Phi(\mathbf{B}_i)$) remains unchanged with varying loadings. The calculated equilibrium forces of the OPT-STMs of two bases $\mathbf{B}_2$={$\mathbf{L}_2$} and $\mathbf{B}_3$={$\mathbf{L}_3$} with opposite loading direction are shown in Fig. 18. By changing the direction of the load combination basis, the magnitude of equilibrium forces remains unchanged while the tensile and compressive members are interchanged. In addition, the STS indices also remain unchanged. This feature guarantees the generated OPT-STMs are applicable for various load combinations in a convenient manner.

Secondly, the generated OPT-STMs $\Phi(\mathbf{B}_i)$ indicate independent load

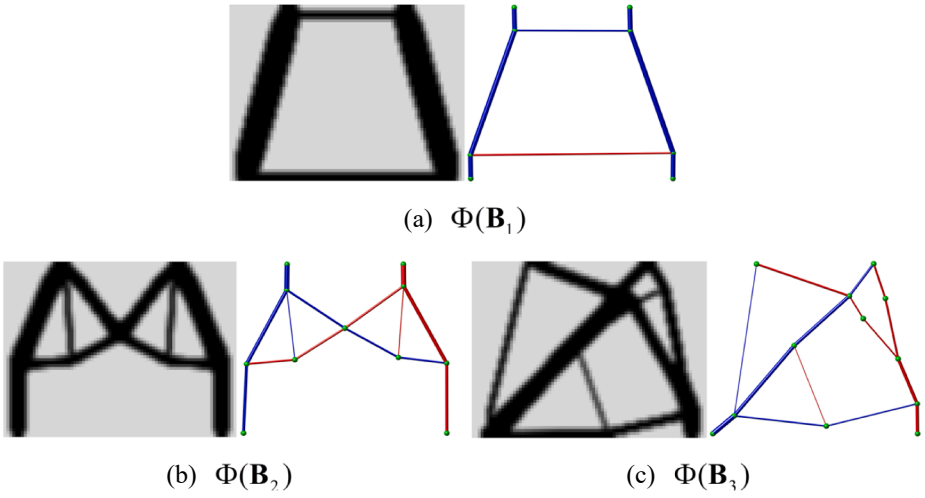

Fig. 16. Topology optimization results and the generated OPT-STMs of the deep beam case.

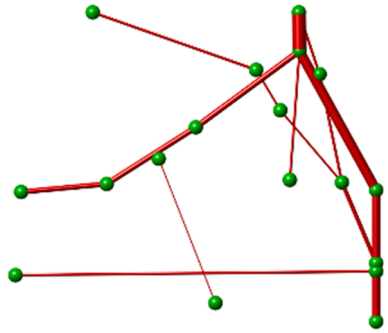

Fig. 17. Required steel cross-sections based on MOST model. Bar width indicates the rebar cross-section.

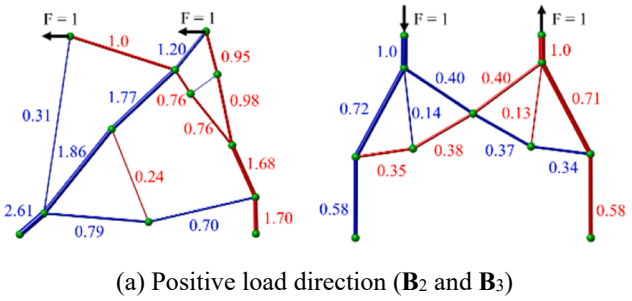

(a) Positive load direction ($\mathbf{B}_2$ and $\mathbf{B}_3$)

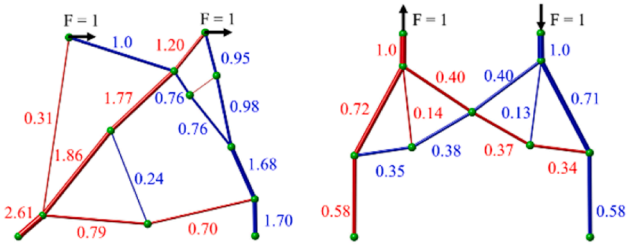

(b) Negative load direction (-$\mathbf{B}_2$ and -$\mathbf{B}_3$)

Fig. 18. Member forces of the OPT-STMs by varying load directions. Red and blue members indicate ties and struts respectively. Bar width indicates the force magnitude. The normalized member forces for a unit loading (F) are presented. (For interpretation of the references to colour in this figure legend, the reader is referred to the web version of this article.)

transfer mechanisms for the corresponding load basis vectors. For the deep beam case, Fig. 19 shows a truss-like structure consisting of three generated OPT- STMs with the same loading points and supports. The calculated member forces with this combined model under three basis vectors $\mathbf{B}_i$ are shown in Fig. 20. Compared to the obtained forces in OPT-STMs (Fig. 16), the combined model shows a similar force distribution and the difference is insignificant. This feature enables that the design of multiple load combinations can be performed via combination of several basic OPT-STMs. In this way, the MOST model provides a uniform design model for all the considered load combinations.

3.5. Performance evaluation and comparison

In order to investigate the performance of the designs based on the four generated models, NLFEA is used to simulate the structural performance. Geometry nonlinearity and material nonlinearities (the cracking and crushing of concrete and the yielding and rupturing of steel) are considered in the NLFEA simulation. In the NLFEA models, we assume that reinforcement bars are located corresponding to the ties in the STM model and their cross-sections are based on full utilization of the yielding stress at the design load. These designs are simulated considering the cracking and crushing of concrete and the yielding and rupturing of steel. For the brevity of this paper, for the detailed modelling choices, settings and solution strategies we refer to our previous studies [47,49]. The obtained loading capacities and total steel usage are used to evaluate the performance of these designs.

Here, we define a factor η to evaluate the ultimate capacity with respect to various load combinations. Since the applied loads are proportional to the considered $i-$ th design load combination, the capacity

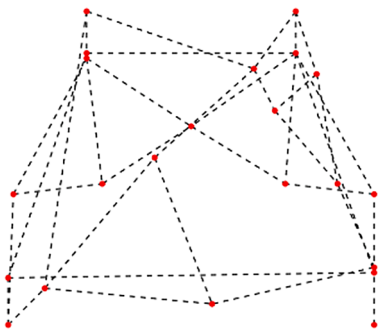

Fig. 19. The combined model based on the three generated OPT-STMs.

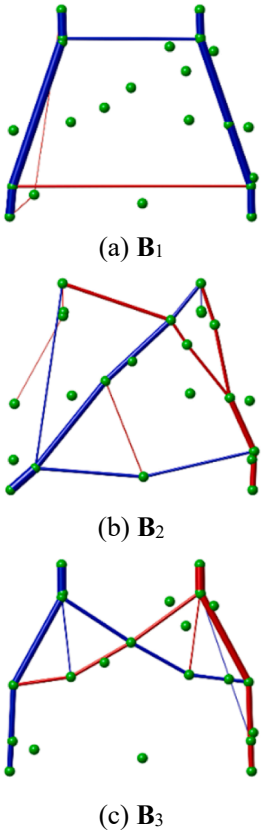

(a) $\mathbf{B}_1$

(b) $\mathbf{B}_2$

(c) $\mathbf{B}_3$

Fig. 20. Obtained member forces based on the combined truss-like model. Red and blue members indicate ties and struts respectively. Bar width indicates the force magnitude. Members with forces lower than 1% of the maximum force are ignored. (For interpretation of the references to colour in this figure legend, the reader is referred to the web version of this article.)

factor η indicates the ratio of ultimate loading situation $f(\mathbf{C}_i)_u$ and design load combination $f(\mathbf{C}_i)$, given as:

$$\eta_i = \frac{f(\mathbf{C}_i)_u}{f(\mathbf{C}_i)} \tag{13}$$

$\eta_i = 1$ would indicate that the designed load capacity of load combination $\mathbf{C}_i$ is exactly found by NLFEA. For the sake of safety, the lower-bound-based STM design is desired to result in $\eta_i > 1$ for all the considered load combinations. In addition, similar to the previously defined ratio PV in Xia et al. [47] which indicates the degree of steel utilization, a ratio PV_{ML} considering multiple load combinations is proposed, given as:

$$PV_{\mathrm{ML}} = \frac{\eta_* V_0}{V_s} \tag{13}$$

where η_* indicates the load capacity of the most unfavourable load combination. V_0 and V_s indicate the volume of the structure and steel, respectively. Note that for the case $\eta_* = 1$, PV_{ML} is the reciprocal of what is known as the reinforcement ratio. For different STM designs, a design with a larger PV_{ML} indicates a more effective result.

The NLFEA models of the designs based on the previously generated models are shown in Fig. 21. The reinforcement is arranged based on the location of ties, and the size of cross-sections is determined by full utilization of steel strength. The structural performance of the designs under the considered load combinations is evaluated. In the simulation, force control is adopted to apply these load combinations.

The simulated results of four designs are summarized in Table 3. The unfavourable load combinations can be observed based on the obtained capacity factors. Comparing the steel usage of the four designs, MOST design leads to the lowest steel usage of 11.31×10^5 mm^3 and the largest PV_{ML} ratio of 179.94. Compared to the MOST design, the designs of the manual model and multiple ST models result in an increase of steel usage by 17 % and 39 %, respectively. The design based on multiple ST models leads to the lowest PV_{ML} ratio of 116.63. The adoption of the ML-TO model causes a similar steel usage and PV_{ML} ratio compared to the MOST design.

Apart from the design based on the multiple OPT-STMs, the capacity factors η for the considered load combinations are larger than 1, which

Table 3
Evaluation results of the four designs for the deep beam. The unit of steel usage is 10^5 mm^3.

Design	Steel	η				PV_{ML}
		$\mathbf{C}_1$	$\mathbf{C}_2$	$\mathbf{C}_3$	$\mathbf{C}_4$	
Manual ①	13.27	2.46	1.04	1.47	1.30	158.5
STMs ②	15.32	2.65	**0.93**	1.22	1.24	116.6
ML-TO ③	11.38	2.46	1.03	1.04	1.18	173.8
MOST ④	**11.31**	2.46	1.25	1.06	1.24	**179.9**

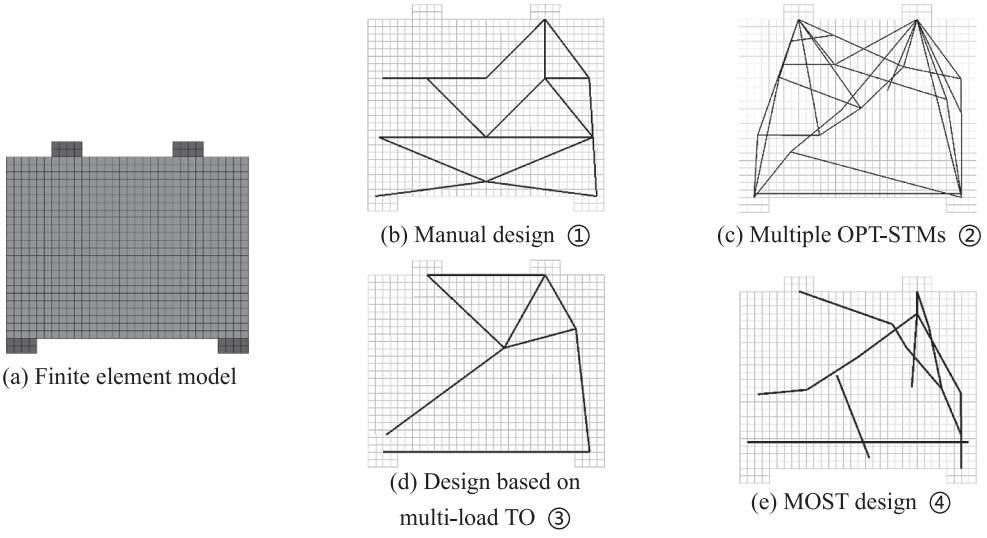

(a) Finite element model

(b) Manual design ①

(c) Multiple OPT-STMs ②

(d) Design based on multi-load TO ③

(e) MOST design ④

Fig. 21. NLFEA model of the four designs of the deep beam considering multiple load combinations. Dark areas in (a) indicates steel loading and support plates. (b) - (e) indicate the resulting rebar location of each design.

indicates safe designs have been obtained. All designs but one fails due to steel rupturing under the considered load combinations. Due to the limited ductility of concrete, the design based on the multiple OPT-STMs results in a lower capacity factor (0.93) even when using much more steel. For the designs based on the manual model, multiple OPT-STMs and the ML-TO model, since the capacity factor η_2 has the lowest values (1.04, 0.93 and 1.03 respectively) compared to other load combinations, $\mathbf{C}_2$ is identified as the unfavourable load combination. Moreover, for the ML-TO model, load combination $\mathbf{C}_3$ is also a critical load combination with $\eta_3 = 1.04$. In contrast, for the MOST design, the unfavourable load combination is $\mathbf{C}_3$ with $\eta_3 = 1.06$. The largest capacity factor η_1 of the four designs indicates a favourable load combination.

Compared to the proposed MOST method, the performance of the design based on ML-TO is slightly worse, slightly more steel is used and the capacity factor of the unfavourable load combination decreases by 0.02. The design based on the manual model uses more steel than the MOST design, however the load capacity in terms of the unfavourable load combination is not improved, which indicates inefficient material usage. The design based on multiple OPT-STMs has the highest steel usage and results in an unsafe design under load combination $\mathbf{C}_2$, which indicates an inaccurate STM model is adopted under multiple load combinations.

In the next section, three other D-regions are investigated. Since some additional shortcomings of the multiple models and ML-TO processes are observed, which will be discussed in Section 5, we mainly compared the MOST model with the manual model for each case.

4. STM designs considering multiple load combinations for 2D and 3D D-regions

In this section, in order to further validate the effectiveness of the proposed method for situations, two 2D D-regions and a 3D D-region under multiple load combinations are investigated. The obtained designs based on the proposed design approach (Approach ④) are compared with the designs based on the manually created models (Approach ①). The reasons methods ② and ③ are omitted from these comparisons will be clarified in Section 5. The first case is a knee joint considering four load combinations. The second case is a tee joint also considering four load combinations. The third case is a 3D knee joint. Compared to the 2D knee joint case, loadings in three mutually perpendicular directions are considered in this case. The investigated D-regions are commonly seen in the beam-column regions of reinforced concrete structures. Due to complex conditions of investigated D-regions, few STM investigations have been reported [46,39,7,22].

4.1. 2D knee joint case

The geometry and boundary conditions of the investigated knee joint are shown in Fig. 22. The thickness of this joint is 400 mm. In this case, three loadings are considered, $\mathbf{L}_1$ and $\mathbf{L}_3$ indicate the vertical load and moment load, respectively. $\mathbf{L}_2$ is the horizontal load caused by possible seismic actions or wind loads. The load magnitude of the considered three loadings is 200 kN (horizontal), 150 kN (vertical) and 90 kN•m (moment), respectively. They are discretized into several concentrated forces at one quarter from the top and bottom of the loaded edge for the STM analysis, as shown in Fig. 22b. In this case, four load combinations are considered, as shown in Table 4.

Three load combination basis vectors $\{\mathbf{B}_i\}$ are obtained, and they are $\{\mathbf{L}_1\}$, $\{\mathbf{L}_2\}$ and $\{\mathbf{L}_3\}$ respectively. The generated ST models corresponding to these basis vectors are shown in Fig. 23. A manually created stable truss model is created for comparison, as shown in Fig. 24. Similar to the previous deep beam case (Section 3), the required reinforcement can be designed. The NLFEA models for these two designs are shown in Fig. 25.

Based on the calculated forces, the steel usage of the two designs based on the MOST model and the manually created ST model is 19.06 $\times 10^5$ mm^3 and 23 66 $\times 10^5$ mm^3. Compared to the manually created ST design, the MOST design achieves a 19 % reduction in steel usage. After simulation of the two designs for the considered load combi- nations, the obtained results are summarized in Table 5. Compared to the manual model, the MOST model results in a larger PV_{ML} ratio of 290.1, indicating a substantially higher steel utilization ratio. All capacity factors of the two designs under the considered load combinations are larger than the design load combination ($\eta > 1$). In this case, load combination $\mathbf{C}_2$ results in the lowest capacity factor of two designs and indicates the unfavourable load combination. In this load combination, a larger capacity margin of the considered load combinations is observed for the MOST design with reduced steel usage. In this case, a safer and more economical design is obtained based on the MOST model.

Note that, the resulting rebar locations of the MOST design are more complex compared to the manual design, which may lead to difficulties in practical steel arrangement and construction. How to consider practical construction aspects in topology optimized ST models is rarely addressed, which is an important future research topic. However, it is out of the scope of the present study.

Table 4
Four considered load combinations of the knee joint.

No.	Load combinations
$\mathbf{C}_1$	$\mathbf{L}_1 + \mathbf{L}_2$
$\mathbf{C}_2$	$\mathbf{L}_1 + \mathbf{L}_3$
$\mathbf{C}_3$	$\mathbf{L}_2 + \mathbf{L}_3$
$\mathbf{C}_4$	$\mathbf{L}_1 + \mathbf{L}_2 + \mathbf{L}_3$

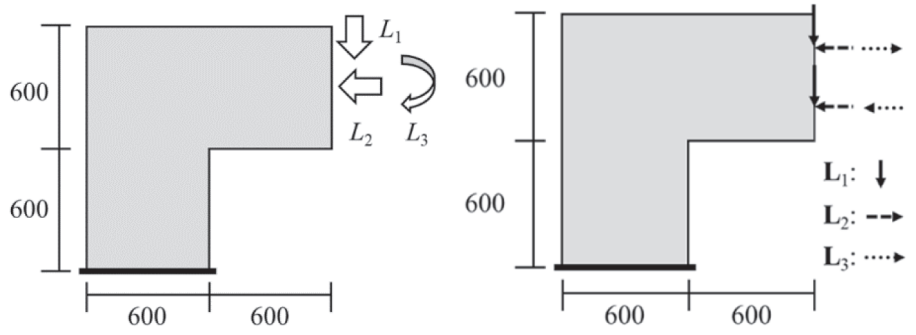

(a) Loading conditions (b) Load discretization

Fig. 22. The geometry, boundary and loadings of the knee joint case (mm).

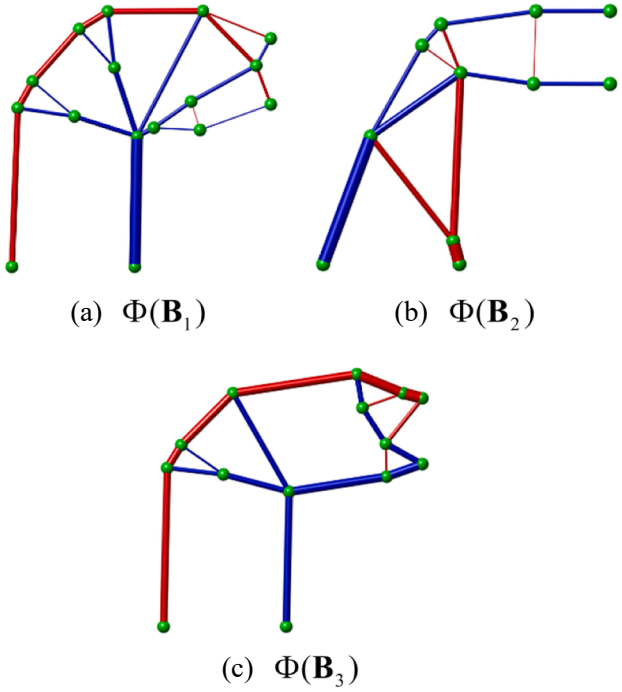

Fig. 23. The obtained OPT-STMs with respect to three basis vectors. Red and blue members indicate ties and struts respectively. Bar size indicates the force magnitude. (For interpretation of the references to colour in this figure legend, the reader is referred to the web version of this article.)

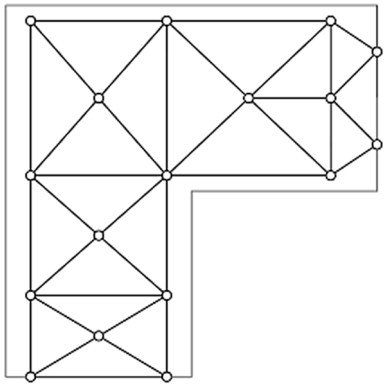

Fig. 24. A manually created ST model considering multiple load combinations.

4.2. 2D tee joint case

The geometry and boundary conditions of the tee joint are shown in Fig. 26. The thickness of this joint is 500 mm. Three loadings are considered for this tee joint. These comprise a moment and a shear force on the left tee joint edge, similar loading on the right tee joint edge, and a horizontal loading acting on both tee joint edges. The resulting discretized loads are shown in Fig. 26, with forces acting at both edges at one tenth from the top and bottom. Loading $\mathbf{L}_1$ represents a vertical load of 200 kN in total and a bending moment of 80 kN•m acting on the left edge, whereas $\mathbf{L}_2$ represents 100 kN on the right edge with the same bending moment (80 kN•m). $\mathbf{L}_3$ represents a horizontal load of 400 kN in total acting on two edges. Four load combinations are considered, as shown in Table 6. For the considered load combinations, three basis vectors $\mathbf{B}_i$ are determined, $\{\mathbf{L}_1\}$, $\{\mathbf{L}_2\}$ and $\{\mathbf{L}_3\}$.

Based on the obtained load combination basis, the corresponding MOST model involving three ST models ($\Phi(\mathbf{B}_i)$) generated, as shown in Fig. 27. A stable truss is manually created for this tee joint as the ST model shown in Fig. 28. Based on the two models, steel is designed to provide sufficient capacity under the considered load combinations. The NLFEA models including the steel arrangement are shown in Fig. 29.

In this case, the steel usage of the MOST and manual ST model is 34.17×10^5 mm^3 and 42.23×10^5 mm^3, respectively. compared to the

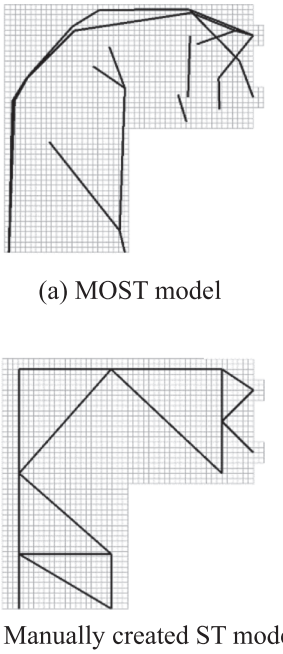

Fig. 25. NLFEA models and the resulting rebar locations of two designs.

Table 5
Evaluation results of the 2D knee joint. The unit of steel usage is 10^5 mm^3.

Design	Steel	η				PV_{ML}
		$\mathbf{C}_1$	$\mathbf{C}_2$	$\mathbf{C}_3$	$\mathbf{C}_4$	
Manual ①	23.66	1.36	1.05	1.22	1.22	191.7
MOST ④	19.06	2.24	1.28	2.20	1.93	290.1

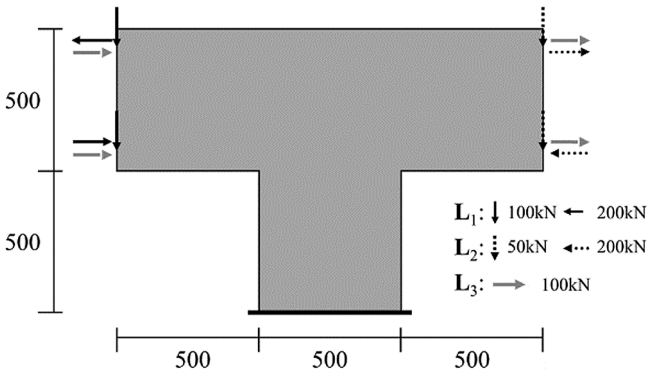

Fig. 26. The geometry, boundary and loadings of the tee joint case (mm).

Table 6
Four considered load combinations of the tee joint.

No.	Load combinations
$\mathbf{C}_1$	$\mathbf{L}_1 + \mathbf{L}_2$
$\mathbf{C}_2$	$\mathbf{L}_1 + \mathbf{L}_3$
$\mathbf{C}_3$	$\mathbf{L}_2 + \mathbf{L}_3$
$\mathbf{C}_4$	$\mathbf{L}_1 + \mathbf{L}_2 + \mathbf{L}_3$

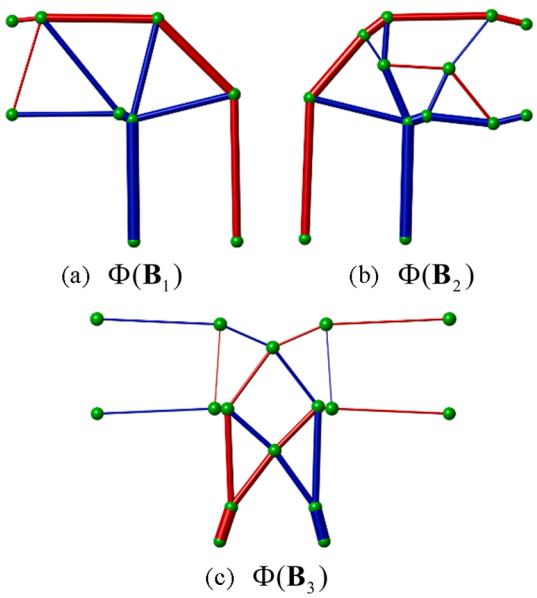

Fig. 27. The obtained MOST model with respect to three basis vectors. Red and blue members indicate ties and struts respectively. Bar size indicates the force magnitude. (For interpretation of the references to colour in this figure legend, the reader is referred to the web version of this article.)

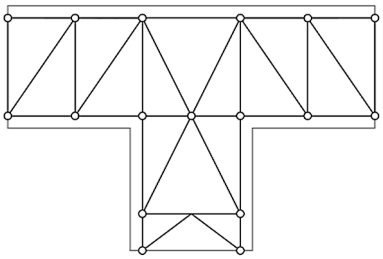

Fig. 28. A manually created ST model considering multiple load combinations.

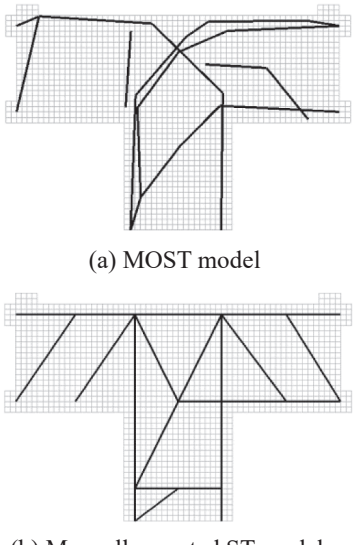

Fig. 29. NLFEA models and the resulting rebar location of two designs.

manually created ST design, the MOST design achieves a 19 % reduction in steel usage. Based on the NLFEA simulated results, the capacity factors η with respect to the considered load combinations are summarized in Table 7. Compared to the manual model, the MOST model results in a larger PV_{ML} ratio of 152.2. Both methods result in safe designs as the capacity factors of all considered load combinations are larger than 1. In this case, for the unfavourable load combination $\mathbf{C}_3$, the capacity margin of the manual STM design is larger than the MOST design, however substantially more steel is required. The MOST model again performs better than the manually created ST model by providing a more economical and effective design, as indicted by the obtained PV_{ML} ratios.

4.3. 3D knee joint case

Referring to the 2D problem in Section 4.1, a similar knee joint in the 3D situation is investigated. The geometry, loading and boundary conditions are shown in Fig. 30. In this case, three loadings are considered, $\mathbf{L}_1$ represents vertical load with a magnitude of 200kN, $\mathbf{L}_2$ and $\mathbf{L}_3$ are horizontal loadings (300kN and 150kN respectively). All loads are discretized with concentrated forces acting at the center of the loaded face. Compared to the 2D case, the 3D case enables investigating the influence of the transverse action ($\mathbf{L}_3$). In this case, six load combinations are considered, as shown in Table 8. Three basis vectors $\mathbf{B}$, $\{\mathbf{L}_1\}$, $\{\mathbf{L}_2\}$ and $\{\mathbf{L}_3\}$, are determined for generating the MOST models.

The obtained MOST model based on the three bases is shown in Fig. 31. Compared to 2D cases, much more computation effort is required in 3D TO. Some measures discussed in our previous work [49], such parallel assembly of the stiffness matrix and reducing redundant DOFs, are taken to speed up the optimization process. The total computation time of this case is about 80 min on a workstation with an Intel i7-10700 CPU and 32 GB memory. For the opposite loading direction ($-\mathbf{L}_1$ and $-\mathbf{L}_3$), the tension and compressive forces in the members of the ST model swap compared to the ST model of $\mathbf{L}_2$ and $\mathbf{L}_3$ while the force magnitude remains unchanged. In order to compare the structural performance, a manually created 3D stable truss is used as the ST model to design the joint under the considered load combinations, as shown in Fig. 32. Similar to the previous cases, steel is designed based on the tensile forces of two designs under different load combinations. The NLFEA models of the two designs are shown in Fig. 33.

The steel usage of the MOST and manual ST model is 47.63×10^5 mm^3 and 53.50×10^5 mm^3 respectively. Based on the simulation results, the capacity factors η and resulting PV_{ML} ratios are summarized in Table 9. Due to the symmetry for the loading $\mathbf{L}_3$, the designs have a similar performance under load combinations $\mathbf{C}_2/\mathbf{C}_4$ and $\mathbf{C}_5/\mathbf{C}_6$, thus from these, only $\mathbf{C}_2$ and $\mathbf{C}_5$ are evaluated. Similar with the previous cases, the design based on the manually created model results in 12 % higher steel usage compared to the MOST design. Both methods result in safe designs, since the load capacity factors are larger than one for the considered load combinations. Again, the MOST model leads to a larger PV_{ML} ratio of 140.1. In addition, the smallest margin of load capacity factors appears in the load combination $\mathbf{C}_3$ which is the unfavourable load situation. Both approaches show a similar safety margin for this case. Load combination $\mathbf{C}_1$ is most the favourable situation. Compared to the 2D case (Section 4.1), based on the obtained model, similar load transfer mechanisms can be observed for the in-plane actions ($\mathbf{L}_1$ and $\mathbf{L}_2$). However, the 3D model provides a more refined design and enables investigating the transverse action ($\mathbf{L}_3$).

Table 7
Evaluation results of the 2D tee joint. The unit of steel usage is 10^5 mm^3.

Design	Steel	η				PV_{ML}
		$\mathbf{C}_1$	$\mathbf{C}_2$	$\mathbf{C}_3$	$\mathbf{C}_4$	
Manual ①	42.23	1.16	1.49	1.07	1.13	126.7
MOST ④	34.17	1.17	1.34	1.04	1.14	152.2

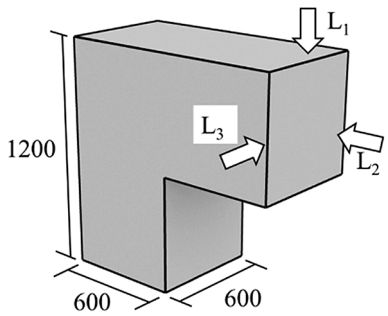

Fig. 30. The geometry, boundary and loadings of the 3D tee joint case (mm).

Table 8
Considered load combinations in designing the 3D knee joint. Symbol - in the load combinations indicates the opposite load direction.

No.	Load combinations
$\mathbf{C}_1$	$\mathbf{L}_1 + \mathbf{L}_2$
$\mathbf{C}_2$	$\mathbf{L}_1 + \mathbf{L}_3$
$\mathbf{C}_3$	$\mathbf{L}_1 - \mathbf{L}_2$
$\mathbf{C}_4$	$\mathbf{L}_1 - \mathbf{L}_3$
$\mathbf{C}_5$	$\mathbf{L}_1 + \mathbf{L}_2 + \mathbf{L}_3$
$\mathbf{C}_6$	$\mathbf{L}_1 - \mathbf{L}_2 - \mathbf{L}_3$

5. Discussion of using multiple ST models and multi-load topology optimization

The previous section focused on a comparison between the proposed MOST method (Approach ④) and the manual approach (Approach ①). In this section, we further investigate the two other procedures for the multi-load STM design problem introduced in Fig. 1, which exhibited certain difficulties that prevented them to be included in the preceding comparisons. These two approaches are applying multiple OPT-STMs with respect to the considered load combinations and applying the multi-load TO formulation (Approach ② and Approach ③ respectively). Through several examples, the features and drawbacks (in terms of applicability and economical aspects) of these two approaches are demonstrated.

5.1. Design based on multiple ST models

Aside from generating manual models, another direct way (Approach ②) to perform STM design considering multiple load combinations is generating multiple models with respect to the considered load combinations. However, this simple procedure was found to have some disadvantages. We will discuss this approach based on the tee joint case of Section 4.2.

For the four considered load combinations $\mathbf{C}_i$, the corresponding OPT-STMs ($\Phi(\mathbf{C}_i)$) are generated independently, shown in Fig. 34. Based on the four models, the total steel usage of the resulting design is 57.97 $\times$ 10^5 mm^3, which 70 % larger than the MOST design (34.17 $\times$ 10^5 mm^3). The evaluation results of this design and the MOST design e summarized in Table 10. Compared to the MOST design, the design based on multiple OPT-STMs leads to a 57% reduction of the PV_{ML} ratio. For the unfavourable load combination $\mathbf{C}_3$, the capacity factor is 1.01 which is smaller than the one of the MOST design (1.04). For load combinations $\mathbf{C}_1$ and $\mathbf{C}_4$, this design results in much larger capacity factors indicating an overly conservative design for these load combinations and a less balanced conservatism with respect to the other two load combinations.

This approach simply generates multiple ST models for designing. The interaction of the considered load combinations is ignored in this

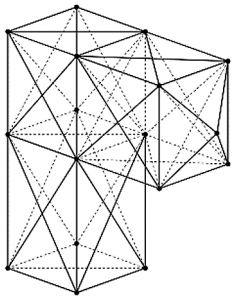

Fig. 32. A manually created ST model suitable for multiple load combinations.

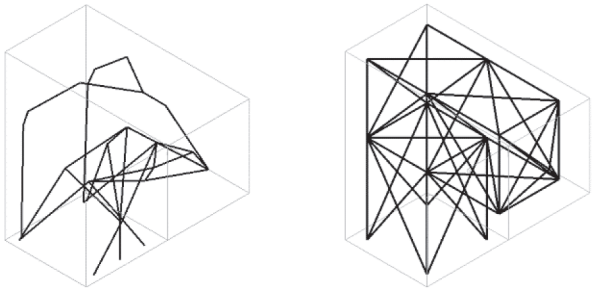

Fig. 33. NLFEA models and the resulting rebar location of two designs.

Table 9
Evaluation results of the 3D knee joint. The unite of steel usage is 10^5 mm^3.

Design	Steel	η				PV_{ML}
		$\mathbf{C}_1$	$\mathbf{C}_2$	$\mathbf{C}_3$	$\mathbf{C}_4$	
Manual ①	53.50	2.05	1.37	1.02	1.63	123.5
MOST ④	47.63	1.70	1.27	1.03	1.39	140.1

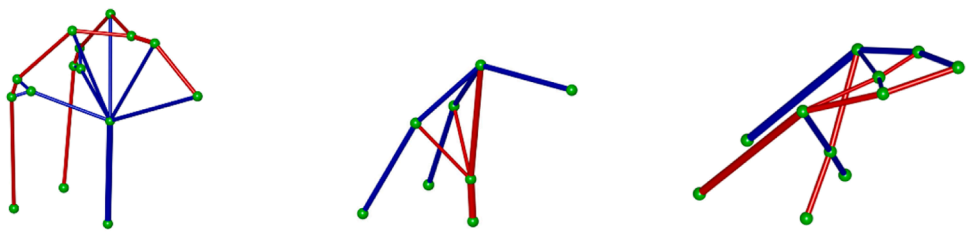

Fig. 31. The obtained MOST models of the 3D knee joint with respect to three load combination bases. Red and blue members indicate ties and struts respectively, and the bar size indicates force magnitude. (For interpretation of the references to colour in this figure legend, the reader is referred to the web version of this article.)

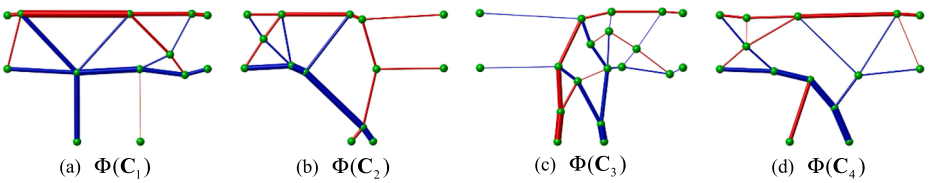

Fig. 34. The obtained OPT-STMs with respect to four considered load combinations of the tee joint case. Red and blue members indicate ties and struts respectively, and the bar size indicates force magnitude.

Table 10
Evaluation results of the tee joint design based on multiple ST models and the MOST model. The unit of steel usage is 10^5 mm^3.

Design	Steel	η				PV_{ML}
		$\mathbf{C}_1$	$\mathbf{C}_2$	$\mathbf{C}_3$	$\mathbf{C}_4$	
STMs ②	57.97	2.31	1.28	1.01	2.35	87.1
MOST ④	34.17	1.17	1.34	1.04	1.14	152.2

method, which leads to more steel usage compared to other approaches. In addition, as the number of considered load combinations increases, more models need to be generated and result in more computational costs compared to the model generation based on load combination basis vectors. For these reasons, this approach based on generating multiple ST models was found to be clearly inferior to other options.

5.2. Difficulties in adopting the multi-load topology optimization formulation

A suitable ST model requires an axial force equilibrium state. For STM generation considering multiple load combinations, the generated models must provide axial equilibrium forces for these combinations. This requirement is achieved by constraining STS indices in the OPT-STM generation process. The satisfaction of STS requirements guarantees the equilibrium state for the considered load combinations. For the application of the ML-TO formulation for STM (Approach ③), the STS requirement may be either not possible or insufficient.

In a relatively simple deep beam case, the shape optimization procedure can obtain suitable models for the considered load combinations for the ML-TO approach. However, for more complex design problems involving more complex (3D) geometry and load situations, the established generation method may be unable to obtain a ST model satisfying all STS requirements. To illustrate this, we perform the generation process for the knee joint case (Section 4.1). The generated model based on the multi-load TO result is shown in Fig. 35a. In this case, the STS indices of the three load combinations are {**0.90**, 0.96, **0.91**, 0.95} respectively. The required axial force equilibrium state cannot be achieved for load combinations $\mathbf{C}_1$ and $\mathbf{C}_3$. Large shear forces are observed in several members, as shown in Fig. 35b. Thus, no valid ST model can

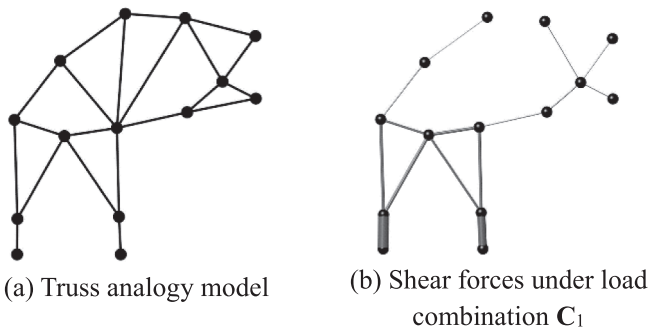

Fig. 35. The generated OPT-STM based on the multi-load TO result of the knee joint case. The bar size indicates the shear force magnitude.

be extracted. This forms a critical issue for using the multi-load based approach in STM under multiple load combinations.

6. Conclusion

In this paper, we propose a method to generate multi-load optimization-based strut-and-tie (MOST) models for STM design problem of reinforced concrete structures considering multiple load combinations. In the proposed method, the load interactions of the considered load combinations are analyzed, and the resulting load combination bases are obtained. Next, several optimization-based strut-and-tie models (OPT-STMs) are generated corresponding to the obtained load combination bases. Combining these OPT-STMs, the MOST model is generated which indicates load transfer mechanisms for the considered load combinations. Axial equilibrium forces can be calculated for the considered load combinations based on the obtained MOST model. Next, the reinforcement is designed based on maximum usage under all the considered load combinations. The proposed method enables automated, systematic multi-load design for both 2D and 3D D-regions. Three 2D D-regions (deep beam, knee joint and tee joint) and a 3D knee joint are investigated and the corresponding MOST models are generated.

In addition to the proposed method, three alternative design procedures are investigated. The first procedure is using the manually created model. The second procedure applies multiple Strut-and-Tie models with respect to the considered load combinations. The last procedure generates Strut-and-Tie models based on the conventional multi- load TO formulation. Nonlinear finite element analysis is used to obtain the structural performance of various designs. The resulting load capacity, steel usage and PV_{ML} ratio (indicating the efficiency of steel usage) are used to compare these designs. Based on the present investigation, the conclusion is summarized as follows:

1. In the investigated cases, the STM designs based on the MOST method produce safe structures, with capacity factors for the considered load combinations larger than 1. Compared to the other three design procedures, the MOST design results in the most economical design (lowest steel usage) and the most effective steel usage (largest PV_{ML} ratio). In the deep beam case, the other three approaches result in an average increase of 25 % in steel usage, without significant improvement of load capacity.
2. The design procedure by combining various OPT-STMs with respect to considered load combinations is a direct way to approach the multi-load STM design problem. However, the interaction of different load combinations is ignored in this process. In the tee joint case, this procedure increases amount of steel by 70 % compared to the MOST design, while the corresponding PV_{ML} ratio reduces by 57 %.
3. The design procedure based on the multi-load TO formulation considers the load interactions in the TO process. however, this procedure lead to difficulties in attaining the required axial force equilibrium. As a result, no model could be generated for use in STM.
4. All considered optimization-based methods lead to reinforcement layouts that pose challenges regarding practical realization. In addition, dynamic loadings are common in the real world. Considering dynamic loading in multiple load combinations is important for

the STM method in practical applications. Inclusion of more constructability and cost aspects and dynamic loadings into the generation process are identified as future research directions.

Declaration of Competing Interest

The authors declare that they have no known competing financial interests or personal relationships that could have appeared to influence the work reported in this paper.

Acknowledgments

The authors would like to thank Prof. Svanberg from KTH, Sweden for providing access to the MMA codes.

Appendix

A. Strut-and-Tie model generation based on multi-load TO

The mathematical formulation of the multi-load SIMP TO method is:

$$\begin{aligned} \min: \quad & g(\boldsymbol{\rho}) = \frac{1}{2}\sum_{i=1}^{n}\beta_i \mathbf{C}_i \boldsymbol{u}_i(\boldsymbol{\rho}) \\ & \boldsymbol{K}(\boldsymbol{\rho})\boldsymbol{u}_i = \mathbf{C}_i \\ \text{s.t.}: \quad & \boldsymbol{V}(\boldsymbol{\rho}) \leqslant \alpha \overline{V} \\ & \boldsymbol{\varepsilon} \leqslant \boldsymbol{\rho} \leqslant 1 \\ & (i = 1, \ldots, n) \end{aligned} \tag{3}$$

Here,g is the total compliance of the structure under n load combinations.$\mathbf{C}_i$ and $\boldsymbol{u}_i$ indicate the nodal force vector and the nodal displacement vector under the i-th load combination, respectively.β_i is the given weight for each load combination. In this paper,β_i stays 1 for all the considered load combinations.

The optimized topology cannot be directly used in STM. Similar to the generation process in Fig. 2, two subsequent steps including topology extraction and STM shape optimization are needed to transform the optimized topology to a suitable ST model, in which the required axial force equilibrium of the considered loadings is obtained. In the shape optimization, since the extracted truss-like structures are statically and kinematically unstable structures, beam elements with high slenderness (height/length $= 10^{-3}$) are used to calculate the equilibrium forces.

However, compared to the STM shape optimization process in Xia et al. [47,48], here the process needs to be modified under multiple load combinations. The mathematical formulation of the STM shape optimization (step 3 in Fig. 2) considering multiple loadings is given by:

$$\begin{aligned} \min: \quad & g(\boldsymbol{x}) = \frac{1}{2}\sum_{i=1}^{n}\beta_i \mathbf{C}_i \boldsymbol{u}_i(\boldsymbol{x}) \\ & \boldsymbol{K}(\boldsymbol{x})\boldsymbol{u}_i = \mathbf{C}_i \\ \text{s.t.}: \quad & S(\boldsymbol{x}) \geqslant 1 - \varepsilon \\ & \boldsymbol{x}_{\min} \leqslant \boldsymbol{x} \leqslant \boldsymbol{x}_{\max} \\ & (i = 1, \ldots, n) \end{aligned} \tag{4}$$

Similar to the multi-load TO formulation,g is the total weighted compliance under n load combinations; $\mathbf{C}_i$ and $\boldsymbol{u}_i$ are nodal forces, and nodal degrees of freedom (displacements and rotations) based on the beam finite element model for the i-th load combination. Here,$\boldsymbol{x}$ indicates the node coordinates of extracted truss structure which are bounded within $\boldsymbol{x}_{\min}$ and $\boldsymbol{x}_{\max}$. Based on the beam element analysis, S_i is the Suitable Truss Structure (STS) index under load combination $\mathbf{C}_i$, which indicates to what extent a purely axially loaded structure has been achieved. Since not all members are significantly loaded under all load combinations, the members which have minor elemental forces are not relevant for the STS index. These inactive members are excluded from the STS calculation. The calculation of the STS index is given by:

$$S = \frac{1}{t}\sum_{e=1}^{t}\frac{|N_e|}{|N_e| + |V_e|}, \tag{5}$$

where,N_e is the element axial force and V_e is the element shear force. t indicates the number of active elements under a given considered load combination. Each element e for which $(|N_e| + |V_e|) \geqslant 0.01\max(|\boldsymbol{N}| + |\boldsymbol{V}|)$ holds (where the maximum is taken over all elements of the structure) is taken as an active element. Since shear forces are inevitable in the beam analysis, similar to Xia et al. [49] a tolerance $\varepsilon = 0.05$ is used in Eq. (4) to relax the STS requirement for the obtained OPT-STMs.

References

[1] Almeida VS, Simonetti HL, Neto LO. Comparative analysis of strut-and-tie models using smooth evolutionary structural optimization. Eng Struct 2013;56:1665–75.
[2] American Association of State Highway Officials and Transportation (AASHTO), 2014. LRFD bridge design specifications, 7th ed. AASHTO, Washington, DC.
[3] American Concrete Institute (ACI), 2008. Building code requirements for structural concrete and commentary. ACI Committee 318-14, Farmington Hills, MI.
[4] Committee A-S-C-E-A-C-I, 445,. Recent approaches to shear design of structural concrete. J Struct Eng 1998;124:1375–417.
[5] Ashour A, Yang K-H. Application of plasticity theory to reinforced concrete deep beams: a review. Mag Concr Res 2008;60(9):657–64.
[6] Bruggi M. Generating strut-and-tie patterns for reinforced concrete structures using topology optimization. Comput Struct 2009;87(23-24):1483–95.
[7] Bruggi M. On the automatic generation of strut and tie patterns under multiple load cases with application to the aseismic design of concrete structures. Adv Struct Eng 2010;13(6):1167–81.
[8] Bruggi M. A numerical method to generate optimal load paths in plain and reinforced concrete structures. Comput Struct 2016;170:26–36.
[9] Canadian Standards Association. Design of concrete structures. Rexdale, Ontario: CSA; 2004.
[10] Chen BS, Hagenberger MJ, Breen JE. Evaluation of strut-and-tie modeling applied to dapped beam with opening. Struct J 2002;99:445–50.

[11] Dey S, Karthik MM. Modelling four-pile cap behaviour using three-dimensional compatibility strut-and-tie method. Eng Struct 2019;198:109499.
[12] El-Metwally S, Chen WF. Structural concrete: strut-and-tie models for unified design. CRC Press; 2017.
[13] European Committee for Standardization (CEN), 2017. Eurocode 2: Design of concrete structures-Part 1-1: General rules and rules for buildings.
[14] fib (International Federation for Structural Concrete). fib model code for concrete structures 2010. Wiley, Lausanne, Switzerland: Ernst & Sohn; 2013.
[15] Gaynor AT, Guest JK, Moen CD. Reinforced concrete force visualization and design using bilinear truss-continuum topology optimiza- tion. J Struct Eng 2013;139(4): 607–18.
[16] Guan H. Strut-and-tie model of deep beams with web openings-an optimization approach. Struct Eng Mech 2005;19(4):361–79.
[17] He Z-Q, Liu Z. Optimal three-dimensional strut-and-tie models for anchorage diaphragms in externally prestressed bridges. Eng Struct 2010;32(8):2057–64.
[18] He ZQ, Liu Z, Ma ZJ. Investigation of load-transfer mechanisms in deep beams and corbels. ACI Struct J 2012;109.
[19] He Z-Q, Xu T, Liu Z. Load-path modeling of pier diaphragms under vertical shear in concrete box-girder bridges. Struct Concr 2020;21(3):949–65.
[20] Herranz UP, Maria HS, Gutiérrez S, Riddell R. Optimal strut-and-tie models using full homogenization optimization method. ACI Struct J 2012;109:605–14.
[21] Jewett JL, Carstensen JV. Experimental investigation of strut-and-tie layouts in deep RC beams designed with hybrid bi-linear topology optimization. Eng Struct 2019;197:109322.
[22] Kassem W. Strut-and-tie modelling for the analysis and design of RC beam-column joints. Mater Struct 2016;49:3459–76.
[23] Kwak HG, Noh SH. Determination of strut-and-tie models using evolutionary structural optimization. Eng Struct 2006;28:1440–9.
[24] Ley MT, Riding KA, Bae S, Breen JE, et al. Experimental verification of strut-and-tie model design method. ACI Struct J 2007;104:749–55.
[25] Liang QQ, Xie YM, Steven GP. Topology optimization of strut-and-tie models in reinforced concrete structures using an evolutionary procedure. ACI Struct J 2000; 97:322–32.
[26] Liang QQ, Xie YM, Steven GP. Topology optimization of strut-and-tie models in reinforced concrete structures using an evolutionary procedure. ACI Struct J 2000; 97.
[27] Liang QQ, Xie YM, Steven GP. Generating optimal strut-and-tie models in prestressed concrete beams by performance-based optimization. ACI Struct J 2001; 98.
[28] Lógó J, Balogh B, Pintér E. Topology optimization considering multiple loading. Comput Struct 2018;207:233–44.
[29] Marti P. Basic tools of reinforced concrete beam design. J Proc 1985;82:46–56.
[30] Mörsch E. Concrete-Steel Construction,(Der Eisenbetonbau), English translation of the 3rd German edition, vol. 33. New York; McGraw-Hill Book Co.: 1909.
[31] Nielsen MP, Hoang LC. Limit analysis and concrete plasticity. CRC Press; 2016.
[32] Park JW, Yindeesuk S, Tjhin T, Kuchma D. Automated finite-element-based validation of structures designed by the strut-and-tie method. J Struct Eng 2010; 136:203–10.
[33] Quintero-Febres CG, Parra-Montesinos G, Wight JK. Strength of struts in deep concrete members designed using strut-and-tie method. ACI Struct J 2006;103:577.
[34] Ritter W. Die bauweise hennebique. Schweizerische Bauzeitung 1899; 33: 59–61.
[35] Schlaich J, Schäfer K. Design and detailing of structural concrete using strut-and-tie models. Struct Eng 1991;69:113–25.
[36] Schlaich J, Schäfer K, Jennewein M. Toward a consistent design of structural concrete. PCI J 1987;32:74–150.
[37] Shobeiri V. Determination of strut-and-tie models for structural concrete under dynamic loads. Can J Civ Eng 2019;46:1090–102.
[38] Shobeiri V, Ahmadi-Nedushan B. Bi-directional evolutionary structural optimization for strut-and-tie modelling of three-dimensional structural concrete. Eng Optim 2017;49:2055–78.
[39] Shyh-Jiann H, Hung-Jen L. Analytical model for predicting shear strengths of interior reinforced concrete beam-column joints for seismic resistance. ACI Struct J 2000;97.
[40] Sigmund O. A 99 line topology optimization code written in matlab. Struct Multidiscip Optim 2001;21:120–7.
[41] Sritharan S. Strut-and-tie analysis of bridge tee joints subjected to seismic actions. J Struct Eng 2005;131:1321–33.
[42] Su RKL, Chandler AM. Design criteria for unified strut and tie models. Prog Struct Mat Eng 2001;3:288–98.
[43] Tjhin TN, Kuchma DA. Computer-based tools for design by strut-and-tie method: advances and challenges. Struct J 2002;99:586–94.
[44] To NHT, Ingham JM, Sritharan S. Strut-and-tie computer modelling of reinforced concrete bridge joint systems. J Earthquake Eng 2003;07:463–93.
[45] Victoria M, Querin OM, Marti P. Generation of strut-and-tie models by topology design using different material properties in tension and compression. Struct Multidiscip Optim 2011;44:247–58.
[46] Vollum RL, Newman JB. Strut and tie models for analysis/design of external beam—column joints. Mag Concr Res 1999;51:415–25.
[47] Xia Y, Langelaar M, Hendriks MAN. Automated optimization-based generation and quantitative evaluation of Strut-and-Tie models. Comput Struct 2020;238:106297.
[48] Xia Y, Langelaar M, Hendriks MAN. A critical evaluation of topology optimization results for strut-and-tie modeling of reinforced concrete. Comput-Aided Civ Infrastruct Eng 2020;35(8):850–69.
[49] Xia Y, Langelaar M, Hendriks MAN. Optimization-based three-dimensional strut-and-tie model generation for reinforced concrete. Comput-Aided Civ Infrastruct Eng 2021;36:526–43.
[50] Yu M, Li J, Ma G. Theorems of limit analysis. Structural plasticity: limit, shakedown and dynamic plastic analyses of structures 2009; 64–73.
[51] Zhou KM, Li X. Topology optimization of structures under multiple load cases using a fiber-reinforced composite material model. Comput Mech 2006;38:163–170.
[52] Zhuang C, Xiong Z, Ding H. A level set method for topology optimization of heat conduction problem under multiple load cases. Comput Methods Appl Mech Eng 2007;196:1074–84.